JOURNAL OF Materials CHEMISTRY

Surface morphology study of corona-poled thin films derived from sol–gel processed organic–inorganic hybrid materials for photonics applications

Yoo Hong Min,[a] Kwang-Sup Lee,*[b] Choon Sup Yoon[a] and Lee Mi Do[c]

[a]*Department of Physics, Korea Advanced Institute of Science and Technology, Taejon 305-701, Korea*

[b]*Department of Macromolecular Science, Hannam University, Taejon 300-791, Korea*

[c]*Electronics and Telecommunications Research Institute, P.O. Box 106, Yusong, Taejon 305-600, Korea*

Dye-doped and a dye-attached sol–gel films using the chromophore (*E*)-*N*-butyl-(4-{2-[4-bis(2-hydroxyethyl)amino]phenyl}-ethenyl)pyridinium tetraphenylborate (BPTP) and *N*,*N*-bis(2-hydroxyethyl)amino-*N*′-methylstibazoliumtoluene-*p*-sulfonate (BAST) were fabricated by sol–gel processing. Surface morphology of the films was studied using an atomic force microscope. In the dye-doped film, many surface defects were observed. The morphology of the surface defects varied as a function of chromophore concentration. The shapes of the defects became more complicated as the chromophore concentration increased. On the other hand, no evidence of such defects was present in the dye-attached film and the quality of the film was high. Also for the dye-attached film, the surface was optically flat and smooth, and the surface roughness was measured to be less than 4 nm. It was found that corona poling processes also affected the quality of the dye-attached film significantly. Corona poling with a needle electrode resulted in many irregular shaped defects in the film. However, poling with a tungsten wire stabilized the corona discharge and thus prevented the formation of defects, which led to films of excellent quality. The electro-optic coefficient, r_{33}, of the BPTP dye-attached film was measured to be 5.0 pm V^{-1} and this value was maintained even after 54 days at room temperature.

Poled side-chain nonlinear optical (NLO) polymers, where organic chromophores with a large molecular hyperpolarizability are covalently bonded to the polymer backbone, have been of great interest for photonics applications.[1] Using such a material, electro-optic modulators with a 40 GHz bandwidth have already been realized at the laboratory level, and a number of passive and active photonic devices were also successfully fabricated.[2]

From the initial stages of NLO polymeric materials research in the mid-1980s, thermal relaxation and low values of NLO coefficients of chromophores in these systems were the major obstacles for practical applications. Since then there have been continuous efforts toward reducing thermal relaxation and increasing the NLO activity of the materials.[3] In recent years, in addition to enhancing these two fundamental factors, the research was extended to improve the optical quality, processability and the chemical stability of NLO materials, which are the properties closely related to those of matrix polymers.

NLO polymer systems which are currently being investigated can be divided into two major categories. These include organic polymer systems with a high glass transition temperature (T_g) polymer as a matrix,[4] and cross-linked inorganic polymer systems.[5] Among inorganic polymers, silicate glass is the most studied and important. It has been reported by several research groups that the use of high T_g polymers can remarkably reduce the thermal relaxation of the molecular dipoles. Such improved stability is attributed to the restricted free volume and the chain stiffness of the polymer matrix. However, it has been pointed out that organic polymers generally produce serious surface damage when poled by the corona discharge method.[6] Using an inorganic polymer, such problems of surface damage can be easily overcome. Silicate glass has a high T_g and also exhibits transparency in the spectral region of device applications, hence it is considered to be an attractive alternative to organic polymer systems.

The sol–gel processing technique is often utilized for fabricating inorganic polymer thin films.[7] Using sol–gel processes, two different types of sol–gel composite films were fabricated in our experiment, namely dye-doped and dye-attached systems. In the former the organic chromophores are physically blended with the silica matrix. The dye-attached system was obtained by using the functionalized silicon alkoxide with one alkoxide functional group substituted by an organic chromophore.

In order to apply these sol–gel films to waveguide devices, the optical propagation loss should be lower than 1 dB cm^{-1}. The causes of optical loss have been attributed to optical absorption, Rayleigh scattering, nonuniform refractive index profile, defects in the film, surface roughness and surface damages generated by corona poling, *etc*.[8] Since these factors are closely related to the method of fabrication, and thus the resulting thin film quality, it is important to assess how different sol–gel processes and corona poling processes affect the parameters mentioned above.

In this work, dye-doped and dye-attached sol–gel films with a stilbazolium salt dye were fabricated. The surface morphologies of the films obtained from different sol–gel processes, curing and poling conditions were investigated using atomic force microscopy (AFM). Surface defects, the electro-optic coefficient and the photobleaching effect are also described.

Experimental

Materials

Tetraethylorthosilicate (TEOS) (Adrich) and 3-isocyanatopropyl triethoxysilane (IP-TEOS) (Lancaster) were used as-received without any further purification. *N*,*N*-Dimethylformamide (DMF) (Junsei) solvent was distilled under reduced pressure over anhydrous magnesium sulfate. The NLO chromophores, (*E*)-*N*-butyl-(4-{2-[4-bis(2-hydroxy-

ethyl)amino]phenyl}ethenyl)pyridinium tetraphenylborate (BPTP) and *N*,*N*-bis(2-hydroxyethyl)amino-*N'*-methylstilbazoliumtoluene-*p*-sulfonate (BAST) were synthesized according to the methods reported elsewhere.[9]

Dye-doped system. TEOS (10.0 g, 48.0 mmol) and ethanol (2.2 g) were mixed in a 40 ml vial with HCl aqueous solution (2.9 g, 2 M), which was added dropwise while stirring gently at 0 °C. Further stirring was performed at room temperature for 12 h by using a magnetic spin bar with a rotation speed of 400 rpm to complete the sol reaction. Then BPTP (0.302 g, 0.457 mmol) and DMF (15 ml) were added to the sol and stirred again until the sol became viscous enough for film casting. Another batch of sol with a different BPTP concentration (0.453 g, 0.686 mmol) was also prepared using the same procedure.

Dye-attached system. DMF solvent (2 ml), IP-TEOS (0.394 g, 1.59 mmol) and BPTP (0.5 g, 0.76 mmol) were mixed together in a 20 ml vial and stirred at 90 °C for 3 h, during which time the bonding reaction of BPTP molecules with IP-TEOS took place to form urethane linkages. After cooling to room temperature, TEOS (0.039 g, 0.189 mmol) and HCl aqueous solution (0.0618 g, 1 M) were added. This mixture was then stirred for 10 days so that an appropriate viscosity for the spin casting might be obtained. Similarly, IP-TEOS (0.221 g, 0.895 mmol) and BAST (0.200 g, 0.425 mmol) were dissolved in DMF (2 ml) and the solution was stirred at 90 °C for 3 h to form urethane bonding between BAST molecules and IP-TEOS. After cooling the solution to room temperature, TEOS (0.0490 g, 0.235 mmol) and HCl aqueous solution (0.0462 g, 1 M) were added and stirred for 15 days for the appropriate viscosity for spin casting to be obtained.

Film casting and corona poling

Sol–gel films were fabricated by the spin casting method. Coating solutions were prepared by the method described in the previous section. The viscous sol was filtered through a Teflon syringe filter of 0.45 μm pore size. Thin films were spin coated on indium tin oxide (ITO) substrates with a rotation speed of 1000–2000 rpm. The film thickness ranged from

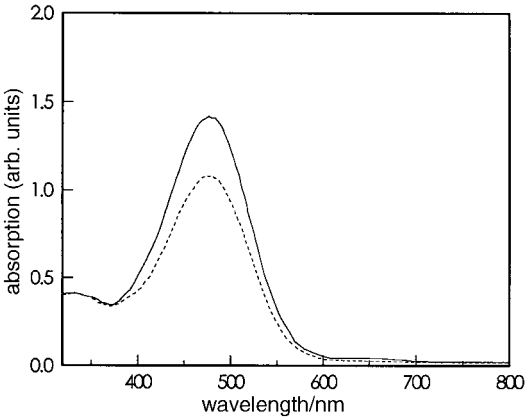

Fig. 2 UV–VIS absorption spectra for cured (———) and poled (----) samples. The poling condition was at 160 °C for 2 h with an applied voltage of 13 kV.

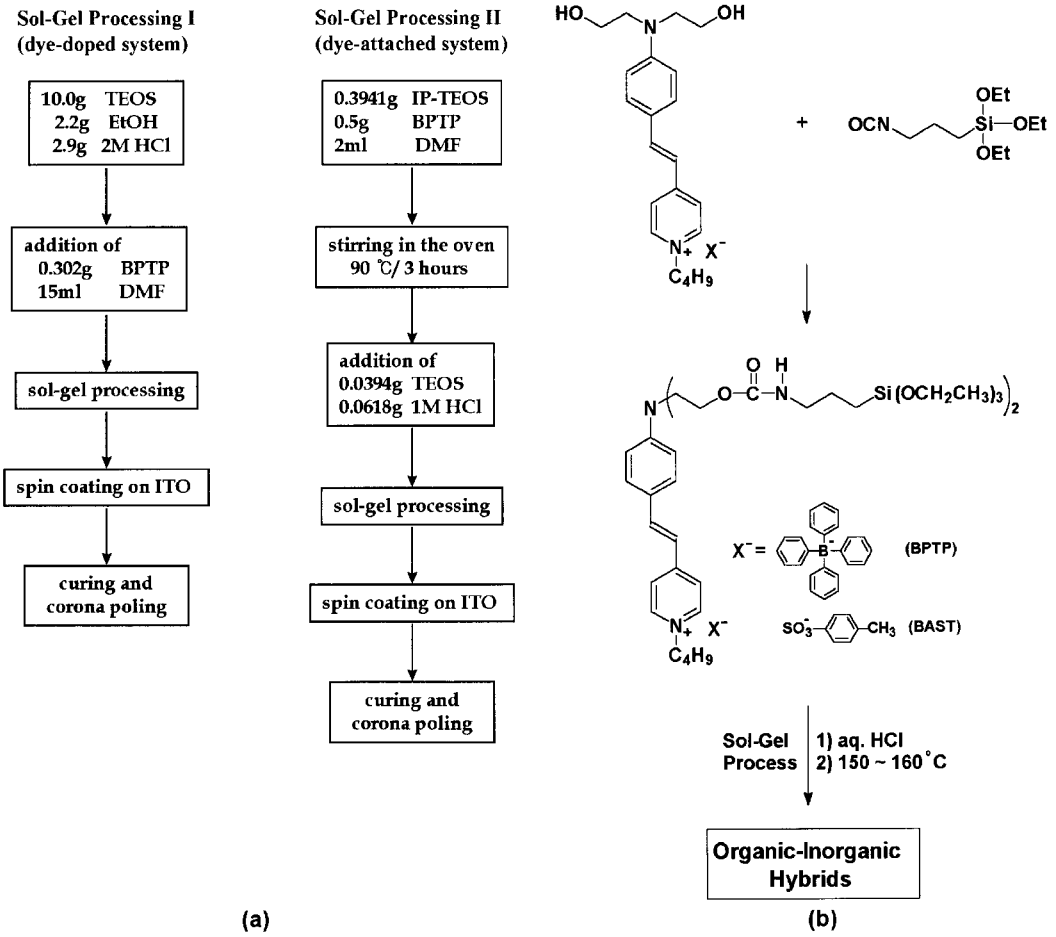

Fig. 1 (a) Two different types of sol–gel routes for dye-doped system (SG-I) and dye-attached system (SG-II). (b) Chemical equation shows the sol–gel monomer for SG-II where the BPTP or BAST salt-type chromophore is covalently bonded to the alkoxysilane by the urethane linkage.

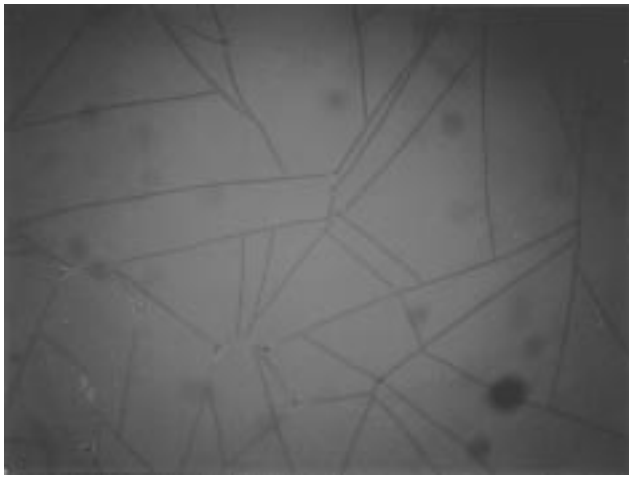

Fig. 3 Optical photograph of a dye-doped sol–gel film (magnification $\times 100$)

0.5 μm to 3 μm for the dye-attached system, depending on the viscosity and the rotation rate. However for the dye-doped system, only films of the thickness less than 1 μm were free of cracks.

The alignment of molecular dipoles in the film was established by the corona poling method. The poling system consisted of a base and an electrode, and the whole system was covered by a glass bell jar. The base was electrically grounded and sat on top of a hot-plate. The atmosphere above the films was not controlled in any way. Either a stainless-steel needle with an edge angle of 60° or a tungsten wire of 20 μm diameter was used as an electrode. In the case of needle poling, the needle electrode was positioned 2 cm above the ground with a poling voltage of 13 kV, at which a stable corona discharge started to be generated. For the wire poling, the distance between the wire electrode and the ground was set at 1 cm and a poling voltage of 5 kV was sufficient for generating a stable corona discharge.

Measurements

UV–VIS spectra were obtained by a Shimadzu UV-3010PC spectrophotometer. The surface morphologies of the films were observed by using a Seiko SPA-300 atomic force microscope (AFM) equipped with an SPI-3700 controller. The 100 μm long cantilever for the AFM (Olympus) was microfabricated from pyramidal Si_3N_4 and the spring constant was 0.09 N m^{-1}. The electro-optic coefficient was measured at 1.3 μm by the simple reflection method proposed by Teng and Man.[10]

Results and Discussion

Two different sol–gel processes for preparing dye-doped and dye-attached systems are shown in Fig. 1. In sol–gel process I (SG-I), the sol–gel film was a physically blended composite where the NLO chromophore was merely distributed in the silica matrix without any chemical attachment. In sol–gel process II (SG-II), the NLO chromophore was covalently bonded to the silica matrix by using the functionalized sol–gel monomer described in Fig. 1(b). Considering the disappearance of the stretching vibration mode peak of the isocyanate group around 2300 cm^{-1} in the FTIR spectrum, the urethane linkage forming reaction between diol of the chromophore and isocyanate of IP-TEOS was assumed to proceed nearly quantitatively.

Fig. 2 shows the UV–VIS absorption spectra for the BPTP dye-attached films prepared by the SG-II process. The spectra were measured in the wavelength range between 250 and 800 nm. Two samples prepared from the same film were used to investigate the poling effect. The absorption maximum for the unpoled film was at 473 nm. For the poled film, the height of the absorption peak was reduced as compared with the unpoled film, but the peak position remained the same. Considering the same curing conditions for both films, the reduction of the peak height can be accounted for by the corona poling effect, which indicates the alignment of chromophore dipoles normal to the film surface.

For the dye-doped system, fabrication of sol–gel films thicker than 1 μm was very difficult because of severe cracking prob-

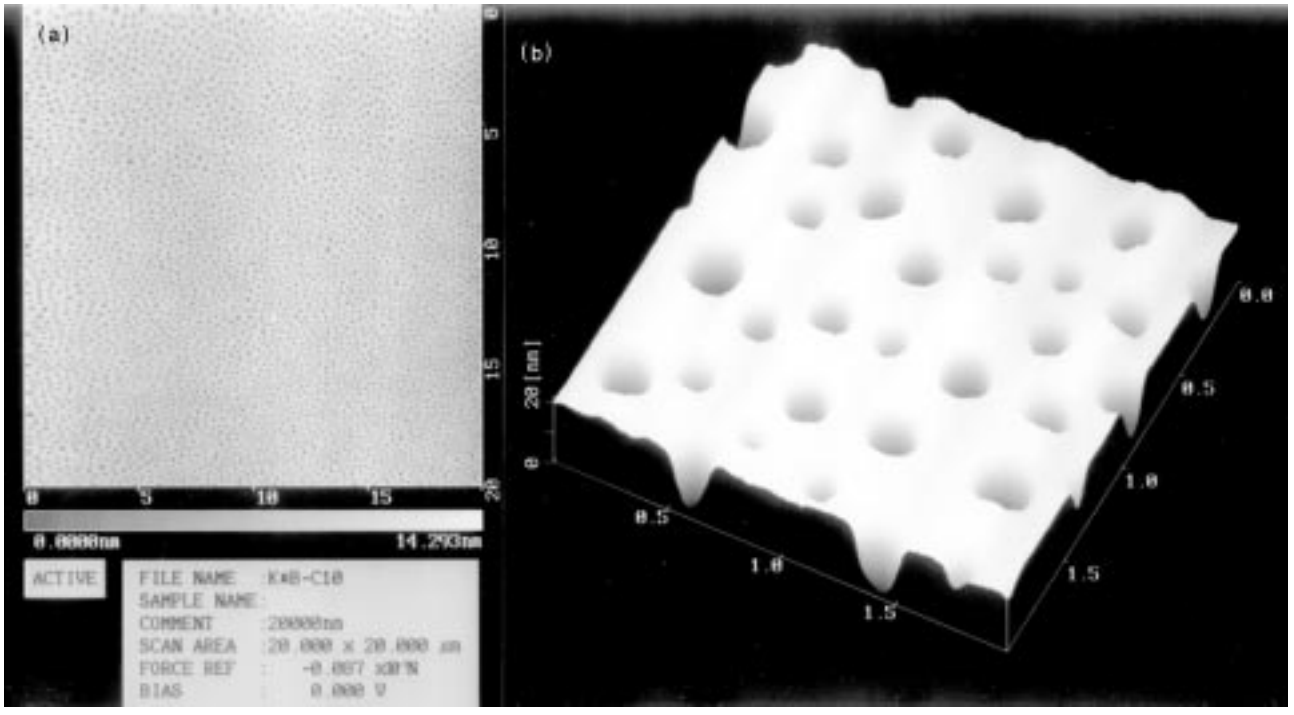

Fig. 4 AFM images of a BPTP dye-doped composite film with 0.46 mmol of BPTP, (a) 20×20 μm^2, (b) 2×2 μm^2. The film was thermally cured at 150 °C for 2 h.

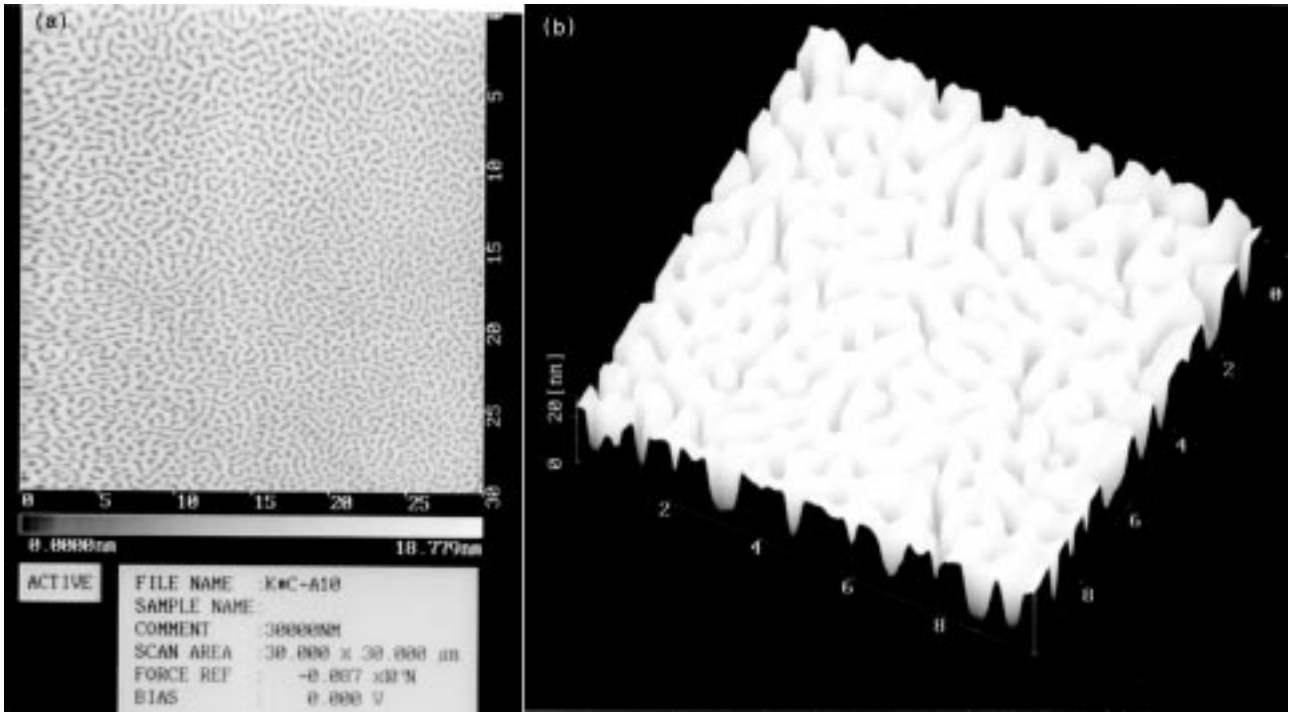

Fig. 5 AFM images of a BPTP dye-doped composite film with 0.69 mmol of BPTP, (a) $30 \times 30\ \mu m^2$, (b) $10 \times 10\ \mu m^2$. The film was thermally cured at 150 °C for 2 h.

lems (Fig. 3). The films were very brittle and the adhesion to the ITO layer was poor. During thermal curing, the color of the dye-doped film changed from bright orange to pale yellow. The melting temperature of the chromophore was 79 °C and decomposition started at around 150 °C, as determined by thermogravimetric analysis (TGA) using a very slow heating run. Therefore, it is very likely that the change in color during the thermal treatment may be caused by decomposition and/or vaporization of chromophore molecules at elevated temperatures.

The AFM images of two dye-doped sol–gel films are shown in Fig. 4 and 5. Both films have the same concentration of TEOS, ethanol and H_2O, and were prepared using the same thermal curing procedures (150 °C for 2 h). The only difference between Fig. 4 and 5 is that the doping concentration of BPTP in the latter was 1.5 times greater than in the former, as was described in the Experimental section (0.46 mmol *versus* 0.69 mmol). In Fig. 4, crater-like defects with diameters of 100–200 nm and a depth of 20 nm were scattered randomly on the surface. On the other hand, in Fig. 5, canyon-like defects run in zigzag fashion, twisted and mingled together. The depth and width of these canyons were less than 20 nm and several hundred nm, respectively, and the length ranged from submicron to several μm. The present result shows that the film quality deteriorated at higher concentrations of BPTP. This may indicate that the distribution of the dye chromophore molecules becomes less inhomogeneous at the nanometer scale as the BPTP concentration increases. The maximum doping ratio of the NLO chromophore without any phase separation was about 5–6 wt.%.[11] Here, no phase separation is defined as there was no observable aggregation of the dye through an optical microscope. Whether or not the distribution of the chromophores in the silica matrix was uniform on the nanometer scale could not be proved. When the concentration of chromophore exceeded a certain critical value, the film was observed to be translucent and surface defects were observed. Fig. 6(a) is the SEM micrograph of the dye-doped film containing BPTP chromophore (20 wt.%). This film was not cured so that the dye aggregations remained on the surface or inside the film. On the other hand, no aggregation was found on the surface of the dye-attached film [Fig. 6(b)].

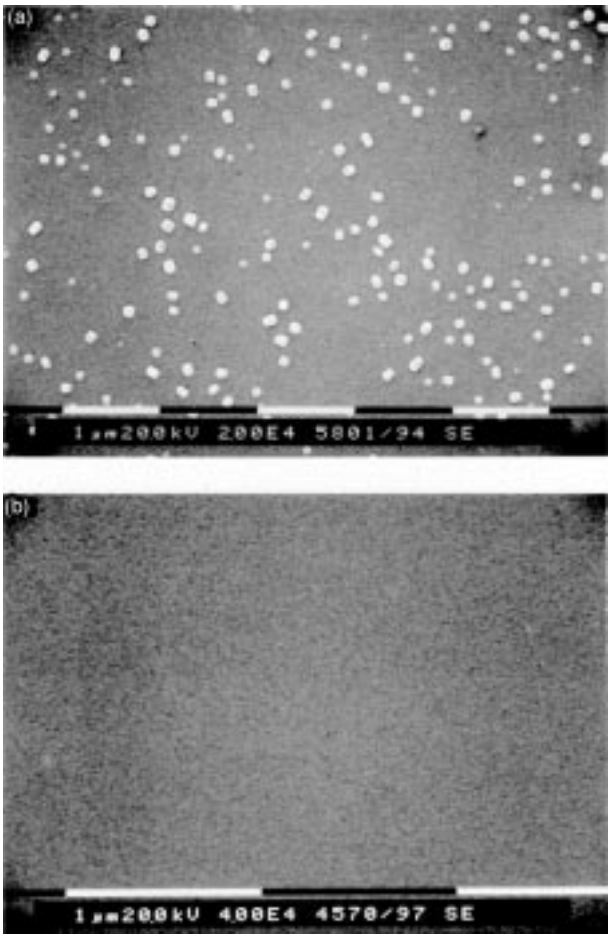

Fig. 6 SEM micrographs for (a) a dye-doped film of 20 wt.% dye concentration and (b) a dye-attached film of 64 wt.% dye concentration

Fig. 7(a) and (b) show the AFM images, at different magnifications, of a BPTP dye-attached sol–gel film fabricated by the SG-II route without corona poling. In this case, the thin film was thermally cured at 160 °C for 80 min. As seen from Fig. 7(a), the surface was relatively flat and defects such as craters or canyons could not be observed. The surface roughness was estimated to be less than 2 nm from AFM images of higher magnification (2×2 μm^2) [Fig. 7(b)]. It is believed that the reasons for the remarkable improvement of the dye-attached film quality were that the chemical bonding of chromophore molecules to the silica matrix prevented the dye molecules from aggregating and that the chromophore molecules provided elasticity between the stiff SiO_2 backbones. Such elasticity can accommodate severe contractions and hence prevent the formation of cracks [Fig. 6(b)].[12] Film thicknesses of 0.5–3 μm could be fabricated in the dye-attached system and no cracks were found after the thermal treatment. As the concentration of the chromophore increased, the film flexibility approached that of organic polymers and the adhesion to the ITO electrode layer also improved.

Fig. 7(c) and (d) shows AFM images at different magnifications of the SG-II sol–gel film which was cured at 160 °C for 80 min while poling at 13 kV with a corona discharge using a needle electrode. Unevenly distributed defects, in the form of irregular-shaped craters characterized by several hundred nm diameters and 12–26 nm depths, were generated. These defects might been formed by the bombardment of nonuniform and unstable plasma produced from the rough edge of the needle. The depths of most craters were smaller than the wavelength of visible light. However, the diameters were much larger than the UV–VIS wavelength. Therefore, the scattering loss by these defects may not be neglected when used as a waveguide.

The dye-attached sol–gel film using the NLO chromophore

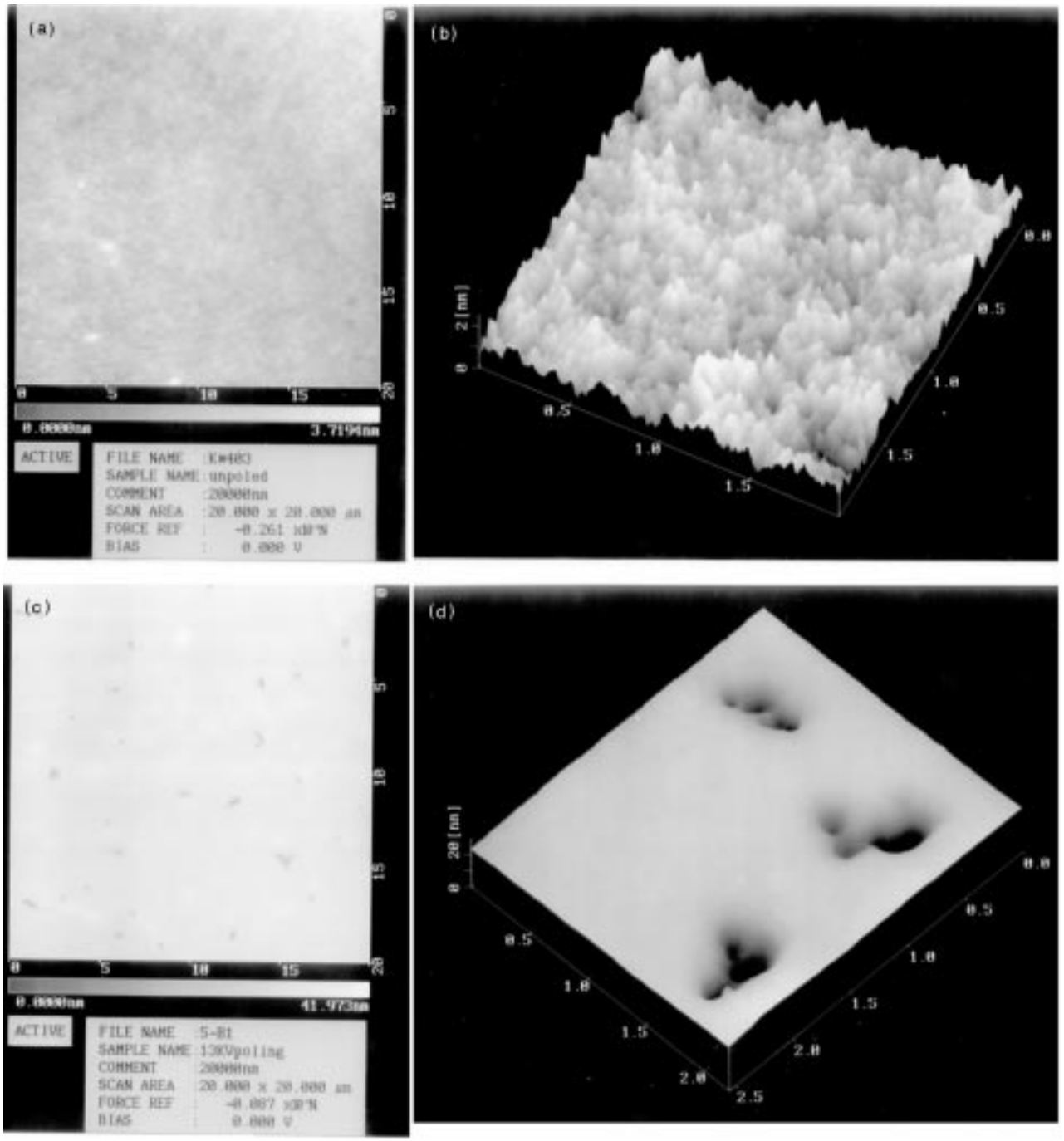

Fig. 7 AFM images of BPTP dye-attached sol–gel composite films: (a,b) without and (c,d) with corona poling using a needle electrode. The image sizes were 20×20 μm^2 for (a,c), 2×2 μm^2 for (b) and 2.5×2.5 μm^2 for (d). The films were thermally cured at 160 °C for 80 min.

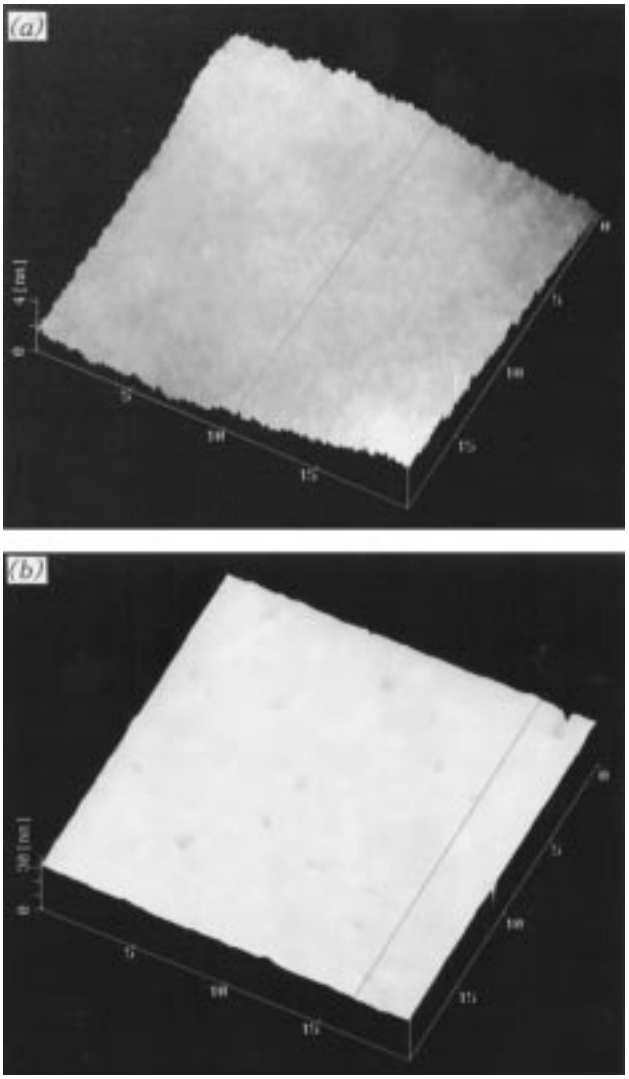

Fig. 8 AFM images ($20 \times 20\ \mu m^2$) of BAST dye-attached sol–gel composite films (a) without and (b) with corona poling using a needle electrode

with tosylate anion (BAST) instead of tetraphenylborate anion was also prepared by the SG-II process. AFM images for two different BAST sol–gel films without and with corona poling using a needle electrode are exhibited in Fig. 8(a) and (b), respectively. The overall surface morphologies show features similar to the BPTP dye-attached sol–gel film. The surface of the cured only film is very flat and smooth [Fig. 8(a)] and the surface roughness is less than 4 nm. However, the AFM images of the BAST thin film, which was corona-poled by using a needle electrode, showed many defects of irregular shapes and sizes similar to those shown by the BPTP film [Fig. 7(c), (d)]. This problem could be overcome by using a tungsten wire electrode. Fig. 9 shows the surface morphology of a 20 μm diameter tungsten wire poled sample and nearly no surface damage can be observed. The results imply that if corona discharge is stabilized by the tungsten wire, it is possible to avoid the surface damage generated by the plasma and poled films of excellent quality can be obtained.

In order to investigate the influence of corona poling on dye-attached films, cross-sectional AFM images were analyzed. As shown in Fig. 10, the surfaces of unpoled BPTP (a) and BAST (b) films are very smooth and flat. In contrast, BAST film (c) poled by the needle electrode has valleys of 3–8 nm depth and 0.8–1.2 nm width, and peaks of 3–4 nm height and 1.5–3 μm width. The results of roughness measurements are summarized in Table 1. The roughness of the BAST thin film, poled by using a needle electrode, was four times greater than those of unpoled BAST and BPTP dye-attached films.

The dye-attached sol–gel film showed a good stability towards stabilized corona discharge. This obviously contrasts with the case of organic polymer systems where severe surface damage, such as cracks, pin holes, chemical reaction, surface deformation, *etc*., was generated.[6] The endurance of the sol–gel film may be due to the strong covalent bonds which forms the SiO_2 matrix.

Electro-optic properties of the poled dye-attached BPTP films were investigated. Measurements on dye-doped films were not possible because of low dye concentration (lower than 5 wt.%), sublimation and/or decomposition of the dye during the poling process, and rapid thermal relaxation. The

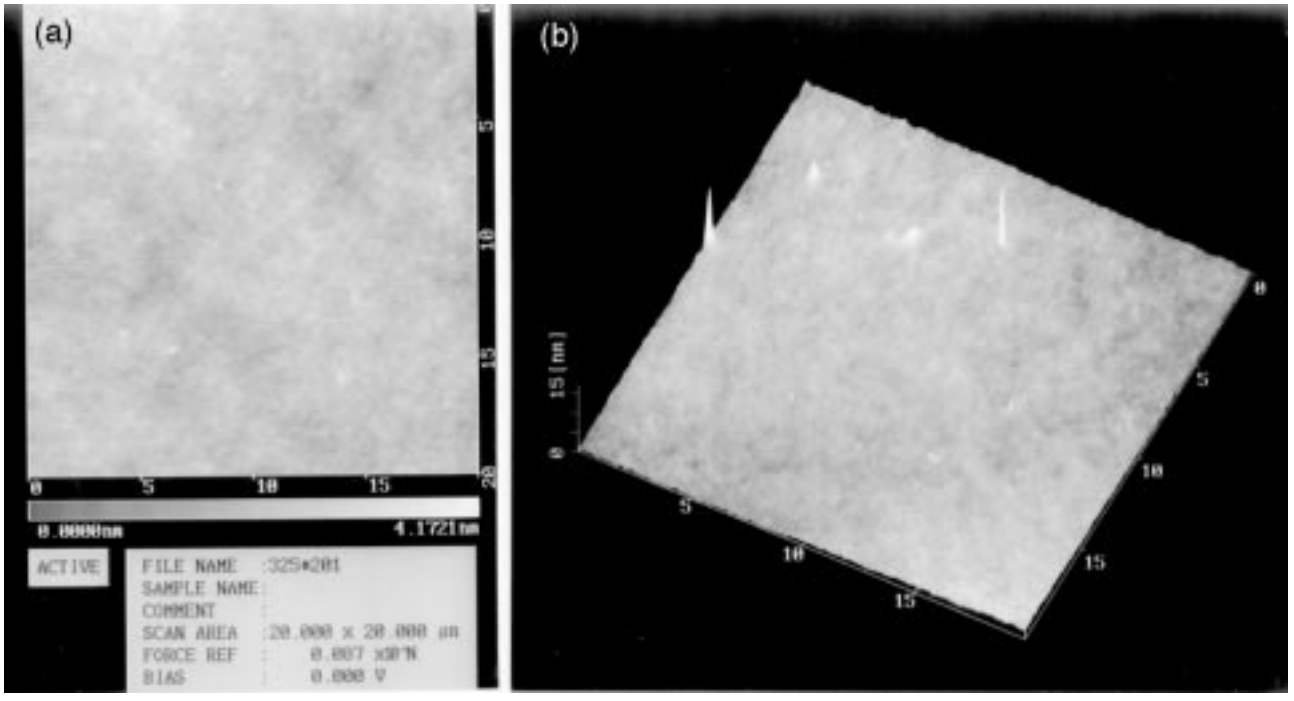

Fig. 9 AFM image ($20 \times 20\ \mu m^2$) of a BAST dye-attached sol–gel composite film. The film was poled with an applied voltage of 13 kV using 20 μm tungsten wire. (a) Top view and (b) inclined side view.

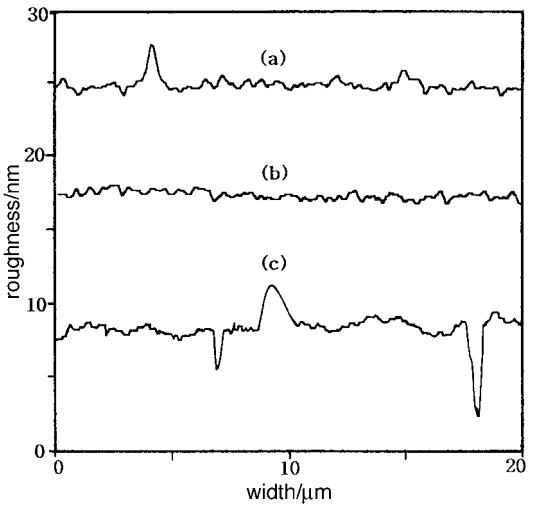

Fig. 10 (a) Cross-section of Fig. 7(a); (b) cross-section of Fig. 8(a); and (c) cross-section of Fig. 8(b)

Table 1 Roughness measurements of dye-attached films

sample	R_a^a/nm	R_{max}^b/nm	R_z^c/nm
Fig. 7(a)	0.209	3.563	1.163
Fig. 8(a)	0.199	1.290	0.866
Fig. 8(b)	1.517	9.480	4.177

[a]The mean roughness (R_a), calculated from $R_a = 1/L\int|f(x)|dx$, with $f(x)$ the profile curve and L the length of the profile curve. [b]R_{max} was obtained from the difference between the highest and lowest points on the profile. [c]R_z was determined, which gives the mean variation between the twenty highest and twenty lowest points on the profile.

electro-optic coefficient, r_{33}, was measured at a wavelength of 1.3 μm for the samples which were poled by a needle electrode at 160 °C for 2 h with an an applied voltage of 13 kV. The electro-optic coefficient values at different sites of a film remained the same inside a circular boundary of about 10 mm diameter. However the electro-optic coefficient values of different films varied between 3.1 and 5.0 pm V^{-1} with the most probable frequency at 4 pm V^{-1}, since the poling efficiency varied greatly from time to time even under the same poling conditions. As shown in Fig. 2 the absorption peak is quite far from the wavelength used for measuring the electro-optic coefficient. Hence the measured electro-optic coefficient can be regarded as a non-resonant value.

In corona poling, conductivity can hardly be quantified because the leakage current, applied electric field and conduction area are not well defined. However an estimation of the conductivity of the film can be made for contact poling. A very large conduction was observed at elevated temperatures over 100 °C, and as a consequence the film was damaged and dc contact poling was not possible. The leakage current was about 100 μA over an electrode area of 30 mm^2 in which the applied field strength was 50 V μm^{-1} which corresponds to a value two orders of magnitude larger than that observed in nonionic organic sol–gel films, such as 4-[*N*,*N*-di(2-hydroxyethyl)amino]-4′-nitrostilbene (DANS diol).

The large electrical conduction observed in the ionic sol–gel films would certainly reduce the poling field by draining the charges piled up on the film surface, and this could lead to a poorer poling efficiency than it might otherwise have. Therefore it is very likely that the electro-optic coefficient values measured were underestimated.

The film showed good temporal stability. The initial value of the electro-optic coefficient remained unchanged for 54 days (Fig. 11).

Photobleaching experiments were performed by using a

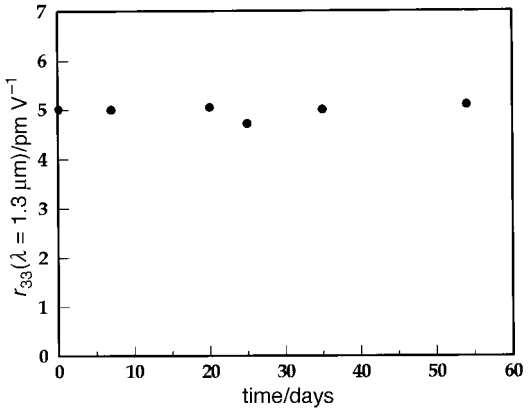

Fig. 11 Temporal stability of the electro-optic coefficient for the SG-II sample at room temperature

large area illuminator (Oriel) as the UV source in the spectral range of 320 to 450 nm. The BPTP dye-attached film was exposed to 55 mW cm^{-1} UV intensity. The change of refractive index was measured at 1.3 μm as a function of exposure time by using a prism coupling method. As shown in Fig. 12, the refractive index decreased exponentially. The refractive index was changed by 0.028 over 3 h exposure. Fig. 13 shows the change of the UV–VIS absorption curve of the photobleached film. The absorption peak height decreased as the exposure time increased. However no new peak appeared as a result of photobleaching. The results suggest that the mechanism of photobleaching in the BPTP chromophore is not due to *cis–trans* isomer transformation, as happens with azo or stil-

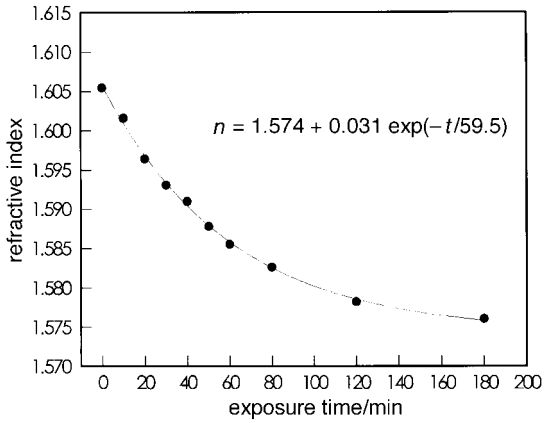

Fig. 12 Change of refractive index of the BPTP dye-attached sol–gel film by photobleaching effects

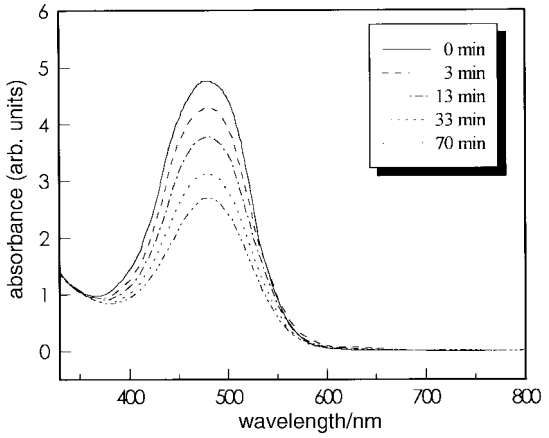

Fig. 13 Change of UV–VIS absorption spectrum of the BPTP dye-attached sol–gel film by photobleaching effects

bene dyes.[13] However, the results support the possibility that the UV radiation could break the double bond of BPTP chromophore molecules, which would then lead to the reduction of charge transfer absorption in the photobleached film.

Conclusions

Using sol–gel processes, a BPTP dye-doped film and BPTP, BAST dye-attached films were fabricated. Surface morphology was studied by using AFM and many surface defects were observed in the dye-doped film. As the chromophore concentration increased, the defect concentration also increased and the shapes of defects became more complicated. On the other hand, surface defects were not observed in the dye-attached sol–gel film. Surface roughness was measured to be less than a few nm. In the film poled by the needle electrode, many defects of irregular shapes were present due to nonuniform distribution of the corona discharge. When the corona discharge was stabilized by a 20 μm diameter tungsten wire electrode, such defects were not observed and poled film of an excellent quality was obtained.

The electro-optic coefficient, r_{33}, of the poled BPTP dye-attached film was measured to be 5 pm V^{-1} and the film exhibited good temporal stability. The initial value of r_{33} remained unchanged even after 54 days at room temperature. A photobleaching experiment was performed with the BPTP dye-attached film and a large refractive index change of 0.028 was induced by UV irradiation of 55 mW cm^{-2} for 3 h.

In summary, the dye-attached organic–silica hybrid films are characterized by excellent temporal stability, controllable refractive index and defect free processability. Hence by making further improvements in their electro-optic coefficient, the dye-attached system may be a potential material for photonics applications.

This research was supported by the Basic Science Research Institute Program, Ministry of Education and in part by the Korea Science and Engineering Foundation through the Opto-Electronics Research Center (KAIST). The authors are grateful to Prof. M. Fujihira of Tokyo Institute of Technology for AFM experiments.

References

1 K.-S. Lee, M. Samoc and P. N. Prasad, in *Comprehensive Polymer Science*, ed. S. L. Aggarwal and S. Russo, Pergamon Press, Oxford, 1992, p. 407; P. N. Prasad and D. J. Williams, *Nonlinear Optical Effects in Molecules and Polymers*, Wiley Interscience, New York, 1991; G. A. Lindsay and K. D. Singer, *Polymers for Second-order Nonlinear Optics*, American Chemical Society, Washington DC, 1995.

2 C. C. Teng, *Appl. Phys. Lett*., 1992, **60**, 1538; D. G. Girton, S. L. Kwiatkowski, G. F. Lipscomb and R. S. Lytel, *Appl. Phys. Lett*., 1991, **58**, 1730.

3 J. W. Wu, J. F. Valley, S. Ermer, E. S. Binkley, J. T. Kenny and R. Lytel, *Appl. Phys. Lett*., 1991, **59**, 2213; D. Yu, A. Gharavi and K. Yu, *Appl. Phys. Lett*., 1995, **66**, 1050; M. Chen, L. R. Dalton, L. Yu, Y. Q. Shi and W. H. Steier, *Macromolecules*, 1992, **25**, 4032.

4 B. K. Mandal, Y. M. Chen, J. Y. Lee, J. Kumar and S. Tripathy, *Appl. Phys. Lett*., 1991, **58**, 3; C. Xu, B. Wu, L. R. Dalton, P. M. Ranon, Y. Shi and W. H. Steier, *Macromolecules*, 1992, **25**, 6716; P. M. Ranon, Y. Shi, W. H. Steier, C. Xu, B. Wu and L. R. Dalton, *Appl. Phys. Lett*., 1993, **62**, 2605; J. A. F. Boogers, P. Th. A. Klaase, J. J. de Vlieger, D. P. W. Alkema and A. H. A. Tinnemans, *Macromolecules*, 1994, **27**, 197; C.-K. Park, J. Zieba, C.-F. Zhao, B. Swedek, W. M. K. P. Wijekoon and P. N. Prasad, *Macromolecules*, 1995, **28**, 3713; K. M. White, D. K. Kitipichai and C. V. Francis, *Appl. Phys. Lett*., 1995, **66**, 3099; Y. Shi, W. H. Steier, L. Yu and L. R. Dalton, *Appl. Phys. Lett*., 1992, **60**, 25; A. K.-Y. Jen, K. J. Drost, Y. Cai, V. P. Rao and L. R. Dalton, *J. Chem. Soc., Chem. Commun*., 1994, 965; T. Verbiest, D. M. Burland, M. C. Jurich, V. Y. Lee, R. D. Miller and W. Volksen, *Macromolecules*, 1995, **28**, 3005; D. Yu, A. Gharavi and L. Yu, *Macromolecules*, 1995, **28**, 784; S.-K. Ham, S.-H. Choi, B.-H. Lee and K. Song, *Polymer* (*Korea*), 1997, **21**, 201; H. K. Kim, I. K. Moon, M. Y. Jin and K.-Y. Choi, *Korea Polym. J*., 1997, **5**, 57.

5 J. Kim, J. L. Plawsky, R. LaPerta and G. M. Korenowsky, *Chem. Mater*., 1992, **4**, 249; Y. Zhang, P. N. Prasad and R. Burzynski, *Chem. Mater*., 1992, **4**, 851; R. J. Jeng, Y. M. Chen, A. K. Jain, J. Kumar and S. K. Tripathy, *Chem. Mater*., 1992, **4**, 1141; R. J. Jeng, Y. M. Chen, A. K. Jain, J. Kumar and S. K. Tripathy, *Chem. Mater*., 1991, **4**, 972; G. H. Hsiue, J. K. Kuo, R. J. Jeng, J. I. Chen, X. L. Tiang, S. Marturunkakul, J. Kumar and S. K. Tripathy, *Chem. Mater*., 1994, **6**, 884; F. Chaput, J.-P. Boilot, D. Riehl and Y. Levy, *SPIE Proc*., 1994, **2288**, 286.

6 R. A. Hill, A. Knoesen and M. A. Mortazavi, *Appl. Phys. Lett*., 1994, **65**, 1733.

7 C. J. Brinker and G. W. Scherer, *Sol–Gel Science*, Academic Press, Boston, 1990; L. C. Klein, *Sol–Gel Optics: Processing and Applications*, Kluwer Academic Press, Boston, 1994; E. J. A. Pope, S. Sakka and L. C. Klein, *Sol–Gel Science and Technology*, American Ceramic Society, Westerville, 1995.

8 T. C. Kowalczyk, T. Kose and K. D. Singer, *J. Appl. Phys*., 1994, **76**, 2505; C. C. Teng, M. A. Mortazavi and G. K. Boudoughian, *Appl. Phys. Lett*., 1995, **66**, 667.

9 K. J. Moon, H.-K. Shim, K.-S. Lee, J. Zieba and P. N. Prasad, *Macromolecules*, 1996, **29**, 861; K. J. Moon, Dissertation, KAIST, Taejon, 1996.

10 C. C. Teng and H. T. Man, *Appl. Phys. Lett*., 1990, **56**, 1734.

11 H.-H. Huang, B. Orler and G. L. Wilkes, *Macromolecules*, 1987, **20**, 1322; M. W. Ellsworth and B. M. Novak, *J. Am. Chem. Soc*., 1991, **113**, 2756; S. Chakrabarti, J. Sahu, M. Chakraborty and H. M. Acharya, *J. Non-Cryst. Solids*, 1994, **180**, 96; H. Kaji, K. Nakanishi and N. Soga, *J. Non-Cryst. Solids*, 1995, **185**, 18.

12 G. Philipp and H. Schmidt, *J. Non-Cryst. Solids*, 1984, **63**, 283; B. Litner, N. Arfsten, H. Dislich, H. Schmidt, G. Phillip and B. Seiferling, *J. Non-Cryst. Solids*, 1988, **100**, 378; H. Schmidt, *J. Non-Cryst. Solids*, 1989, **112**, 419.

13 Y. Shi, W. H. Steier, L. Yu, M. Chen and L. R. Dalton, *Appl. Phys. Lett*., 1991, **58**, 1131; M. B. J. Diemer, F. M. Suyten, E. S. Trommel, A. McDonach, J. M. Copeland, L. W. Jenneskens and W. H. G. Horsthus, *Electron. Lett*., 1990, **26**, 379.

Paper 8/00917A; *Received* 3rd *February*, 1998